

**Lymphoproliferation, immunodeficiency and early-onset inflammatory bowel disease associated with a novel mutation in Caspase 8**

Veronika Kanderova,<sup>1</sup> Hana Grombirikova,<sup>2</sup> Irena Zentsova,<sup>3</sup> Kamila Reblova,<sup>4</sup> Adam Klocperk,<sup>3</sup> Martina Fejtikova,<sup>1</sup> Marketa Bloomfield,<sup>3</sup> Barbora Ravcukova,<sup>2</sup> Tomas Kalina,<sup>1</sup> Tomas Freiburger<sup>2,4</sup> and Anna Sediva<sup>3</sup>

TF and AS contributed equally to this work.

<sup>1</sup>Department of Pediatric Hematology and Oncology, 2<sup>nd</sup> Faculty of Medicine, Charles University, and University Hospital Motol, Prague; <sup>2</sup>Centre for Cardiovascular Surgery and Transplantation, Brno; <sup>3</sup>Department of Immunology, 2<sup>nd</sup> Faculty of Medicine, Charles University and University Hospital Motol, Prague and <sup>4</sup>Central European Institute of Technology and Medical Faculty, Masaryk University, Brno, Czech Republic

Correspondence: [anna.sediva@fmotol.cz](mailto:anna.sediva@fmotol.cz)  
doi:10.3324/haematol.2018.201673

**Supplementary Table 1.** Immunological characteristics of the *CASP8 c.1232C>T* patient.

Cell Population	Frequency; cells/ $\mu$ l	Reference values
Leukocytes (cells/ $\mu$ l)	10300	4500 - 13500
Lymphocytes (cells/ $\mu$ l)	4190	1100 - 6500
Neutrophils (cells/ $\mu$ l)	4780	2000 - 9600
Monocytes (cells/ $\mu$ l)	730	0 - 1200
Eosinophils (cells/ $\mu$ l)	450	0 - 1000
CD3+ T cells (% lymphocytes; cells/ $\mu$ l)	82 ; 3436	56 - 84 ; 1000 - 2200
CD3+ CD4+ T cells (% lymphocytes; cells/ $\mu$ l)	30 ; 1257	31 - 52 ; 530 - 1300
CD3+ CD8+ T cells (% lymphocytes; cells/ $\mu$ l)	51 ; 2137	18 - 35 ; 330 - 920
Naïve CD4+ (% CD4+ T cells ; cells/ $\mu$ l) (CD3+CD4+CD45RA+CD27+)	14.3 ; 180	37 - 97 ; 200 - 1700
Central memory CD4+ (% CD4+ T cells) (CD3+CD4+CD45RA-CD27+)	10.1	13 - 76
Effector memory CD4+ (% CD4+ T cells ; cells/ $\mu$ l) (CD3+CD4+CD45RA-CD27-)	70.3 ; 884	0.49 - 25 ; 5.1 - 210
Terminally diff. CD4 (% CD4+ T cells) (CD3+CD4+CD45RA+CD27-)	3.3	0.0042 - 5.8
Naïve CD8+ (% CD8+ T cells ; cells/ $\mu$ l) (CD3+CD8+CD45RA+CD27+)	3.3 ; 71	20 - 95 ; 78 - 640
Central memory CD8+ (% CD8+ T cells) (CD3+CD8+CD45RA-CD27+)	1.2	0.42 - 18
Effector memory CD8+ (% CD8+ T cells; cells/ $\mu$ l) (CD3+CD8+CD45RA-CD27-)	72.1 ; 1541	4 - 100 ; 16 - 810
Terminally diff. CD8+ (% CD8+ T cells) (CD3+CD8+CD45RA+CD27-)	21.5	9 - 65
CD3+TCRab+CD4-CD8- T cells (% CD3+ T cells ; % lymphocytes)	0.52 ; 0.44	< 3.5 ; < 2
% HLA-DR / CD3+4+ T cells	61	N/A
% HLA-DR / CD3+8+ T cells	73	N/A
CD19+ B cells (% lymphocytes; cells/ $\mu$ l)	9.3 ; 390	6 - 23 ; 110 - 570
Naïve (% B cells) (CD19+CD27-IgD+)	92.4	51.3 - 82.5
Switched memory (% B cells) (CD19+CD27+IgD-)	1.9	8.7 - 25.6
Plasmablasts (% B cells) (CD19+CD27++CD38++)	0.3	0.6 - 6.5
Transitionals (% B cells) (CD19+CD27-CD24++CD38++)	22.4	1.4 - 13
Marginal zone-like (% B cells) (CD19+CD27+IgD+)	4.8	4.6 - 18.2
NK cells (% lymphocytes; cells/ $\mu$ l) (CD3-CD16+56+)	5.5 ; 230	3-22 ; 70-480
Regulatory T cells (% T cells) (CD4+CD25+CD127+)	4.94	3 - 10
<b>Immunoglobulins</b>		
IgG (g/l)	10.3	7.31 - 12.75
IgG1(g/l)	8.28	3.7 - 12.8
IgG2 (g/l)	1.11	1.06 - 6.1
IgG3(g/l)	0.810	0.18 - 1.63
IgG4 (g/l)	0.215	0.04 - 2.3
IgA (g/l)	0.78	0.91 - 1.7
IgM (g/l)	0.18	0.47 - 1.8
Autoantibodies (ANA, ENA, ANCA, ASCA, RF, CCP, CIK)	negative	
CRP (mg/l)	6	0 - 8

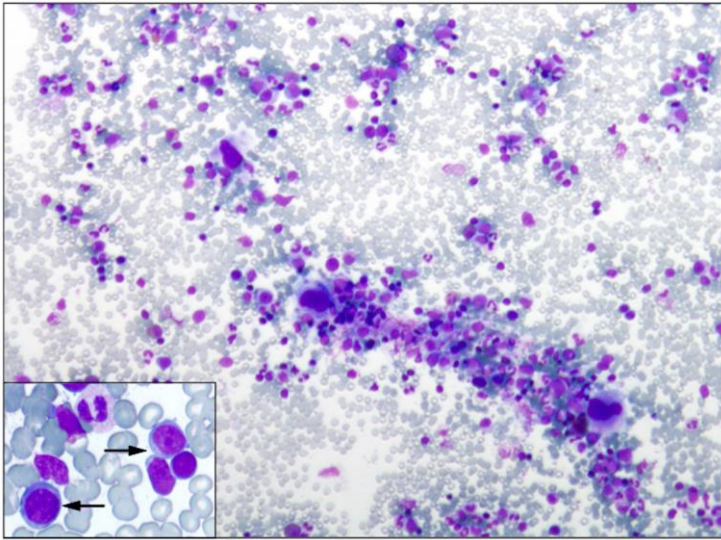
**Supplementary Table 2.** Prediction of the functional effect of variants in the *CASP8* gene.

Variant		Region	Region function	Prediction tools				
cDNA	Protein			CADD	DANN	PolyPhen-2	SIFT	Provean
c.1232C>T	p.P411L	exonic	nonsynonymous	neutral 18.2	deleterious 0.9984	probably damaging 1.0	damaging 0.000	deleterious -8.61
c.793C>T	p.R265W	exonic	nonsynonymous	deleterious 26.9	deleterious 0.9983	probably damaging 1.0	damaging 0.002	deleterious -3.43

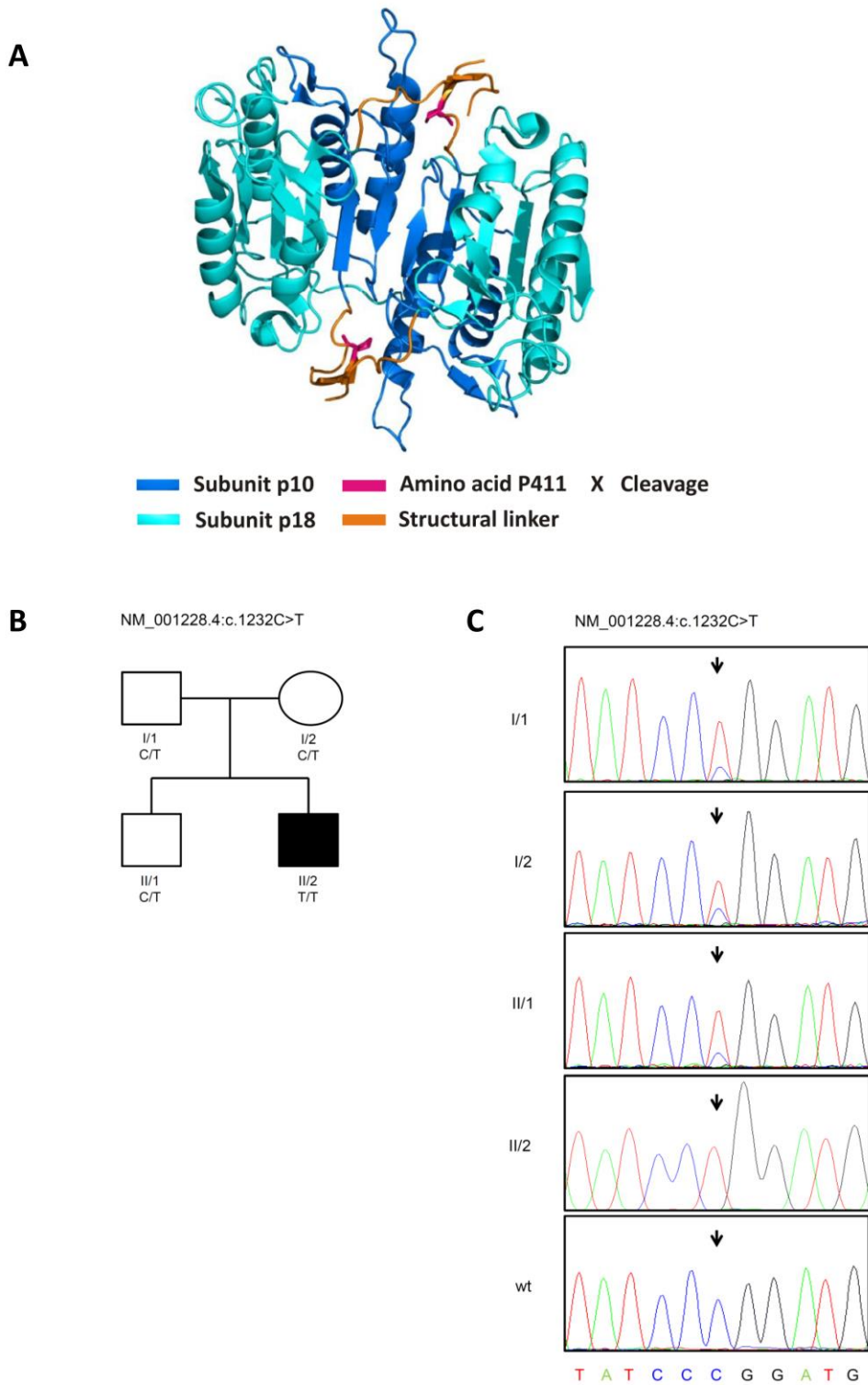
**Supplementary Table 3.** Comparison of the clinical manifestation of the *CASP8 c.1232C>T* patient with the published cases.

Clinical symptoms	Index patient	Chun et al. Pt 1	Chun et al. Pt 2	Niemela et al. Pt 1	Niemela et al. Pt 2*
Sex	male	female	male	female	male
Age at study (years)	15	12	11	42	41
Failure to thrive	+	+	+	-	-
Lymphadenopathy	+	+	+	-	-
Splenomegaly	+	+	+	-	+
Eczema	-	+	+	-	-
Chronic diarrhoea	+	-	+	-	-
Perianal fistula/ rectal prolapse	+	-	-	-	-
Asthma	-	+	+	-	-
Pneumonia	+	+	+	+	+
Recurrent sinopulmonary infections	+	+	+	NR	+
Lung disease	Chronic atelectasis	NR	NR	Interstitial lung disease with lymphoid clusters, necrotizing and non-necrotizing granulomas	Bronchiectasis
Neurologic symptoms	-	-	-	-	Multiple cranial nerves palsy/paresis, necrotizing granuloma in CNS
EBV-related complications	Chronic active EBV infection	-	-	Pancytopenia	-
Other severe/recurrent infections	CMV colitis, Adenoviral pneumonia, Haemophilus infl. pneumonia	HSV labialis	HSV labialis	Nocardia asteroides meningoencephalitis	Staphylococcus aureus and Pseudomonas aeruginosa pneumonias
Serum Ig					
IgG (mg/dl)	1030 (731-1275)	857 (723-1685)	544 (723-1685)	1124 (700-1600)	1030 (700-1600)
IgA (mg/dl)	78 (91-170)	112 (81-463)	56 (81-463)	117 (70-400)	181 (70-400)
IgM (mg/dl)	18 (47-180)	52 (48-271)	32 (48-271)	15 (40-230)	22 (40-230)
IgE (IU/ml)	3 (<200)	7 (<180)	20 (<180)	17 (<380)	46 (<380)
Response to pneumococcal vaccine	poor	poor	poor	ND	ND

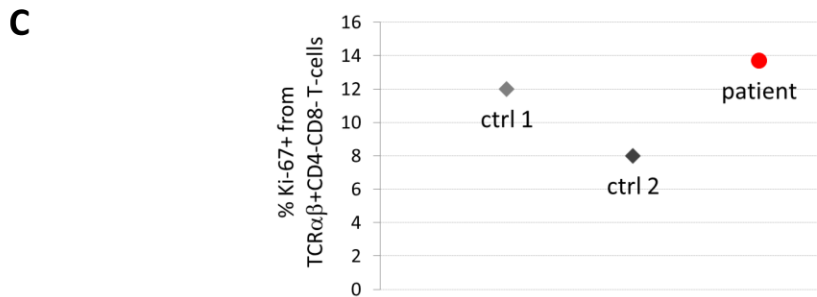
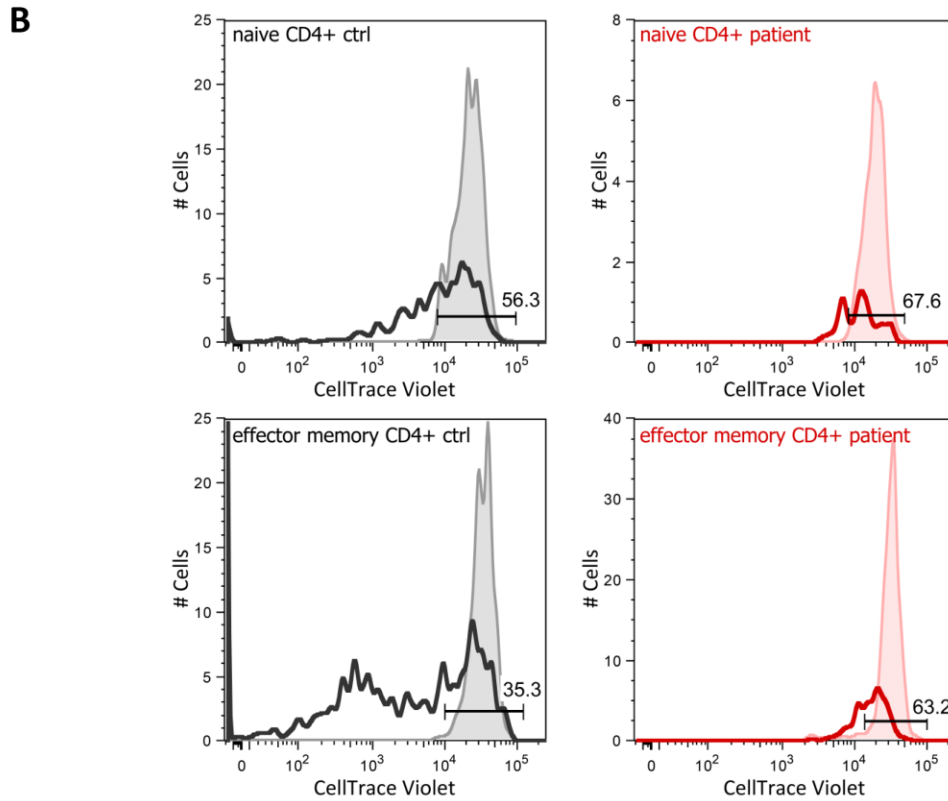
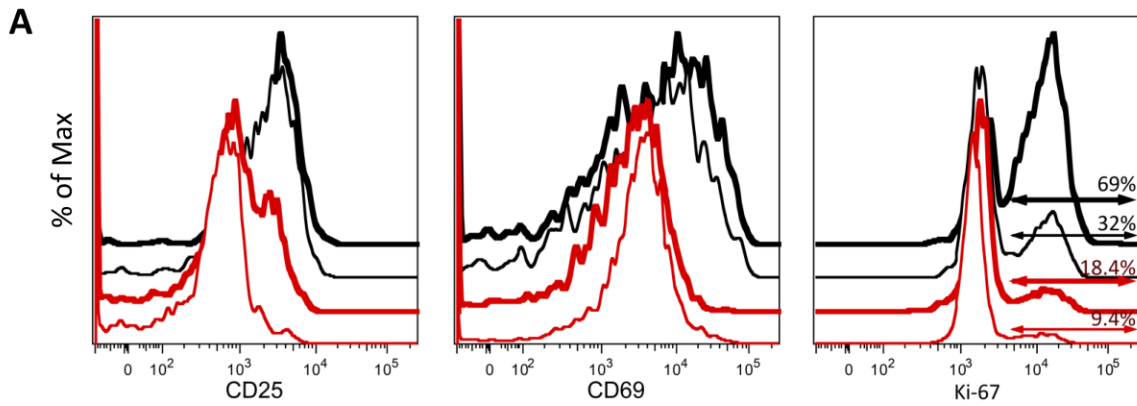
NR - not reported, ND - not done, \*measured on IVIG replacement (600 mg/kg/month)



**Supplementary Figure 1.** Bone marrow aspiration smears. Normocellular bone marrow with maturing trilineage hematopoiesis, arrows indicate reactive lymphocytes (Wright-Giemsa, original magnification x20, inset x100).

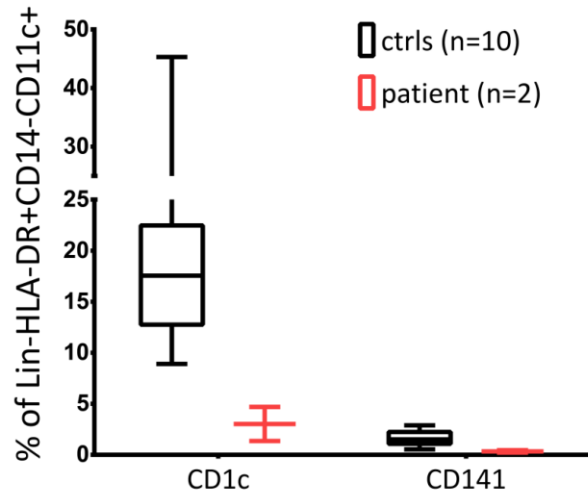


**Supplementary Figure 2. Caspase-8 structure and Sanger sequencing of the *CASP8* substitution variant NM\_001228:c.1232C>T, p.P411L.** **A.** X-ray structure of the caspase-8 dimer after cleavage of the 12 amino acid region in the linker (PDB code 1F9E, Blanchard et al. 2000). Amino acid P411 is positioned in the linker which is part of the dimerization interface. **B.** A pedigree of the patient. **C.** Sanger sequencing confirmed the homozygous variant in the patient and found the same variant in the heterozygous form in his parents and his brother. Arrows show the variant position.



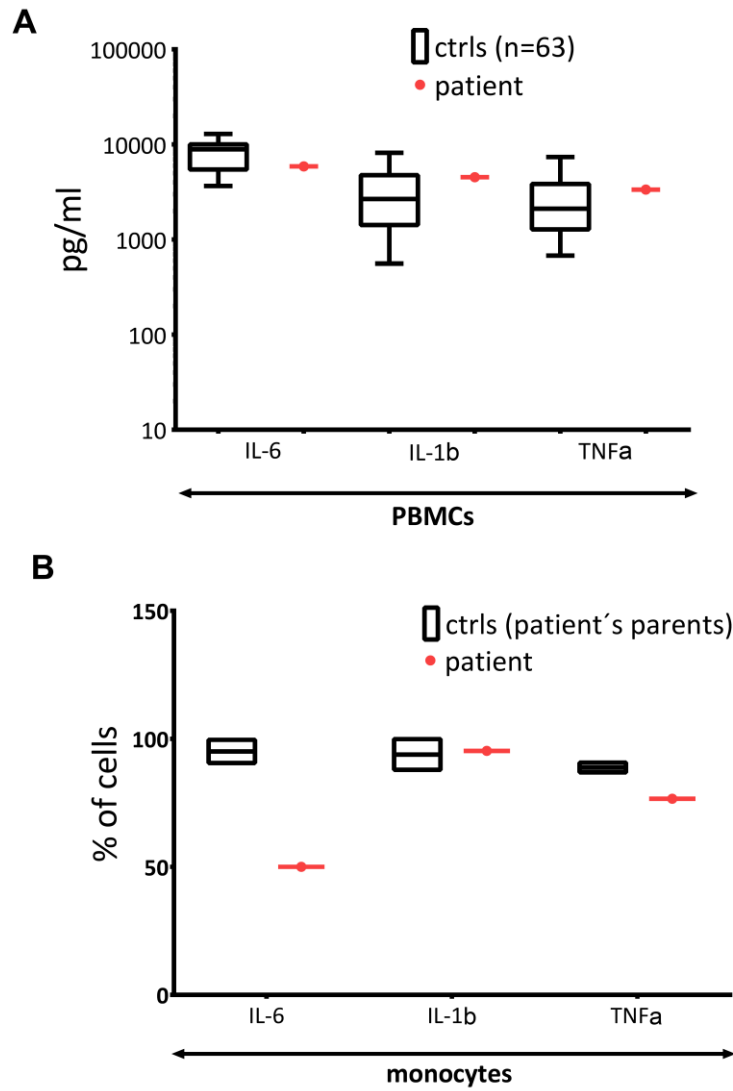
**Supplementary Figure 3. A. Impaired activation and proliferation of patient's CD4+ and CD8+ T cells.** The patient's T cells expressed a lower level of CD25 and CD69 activation markers and demonstrated lower proliferation rate (% Ki-67+, arrows), which were induced by anti-CD3/CD28 stimulation. The addition of interleukin-2 (IL-2, bold) partially rescued CD25 and Ki-67. The result is representative of three independent experiments. CD3+CD8+ T cells are shown 72 hours after TCR stimulation. **B.** The patient's T cells demonstrated low proliferation upon anti-CD3/CD28 stimulation both in

naïve CCR7+CD45RA+ and effector memory CCR7-CD45RA- compartments. The result is representative of two independent experiments performed in duplicates. CD3+CD4+ T cells are shown 6 days after TCR stimulation (bold), tinted graphs represent unstimulated cells. **C.** The patient's double negative TCR $\alpha\beta$ +CD4-CD8- T cells showed comparable basal Ki-67 expression as two independent healthy controls.

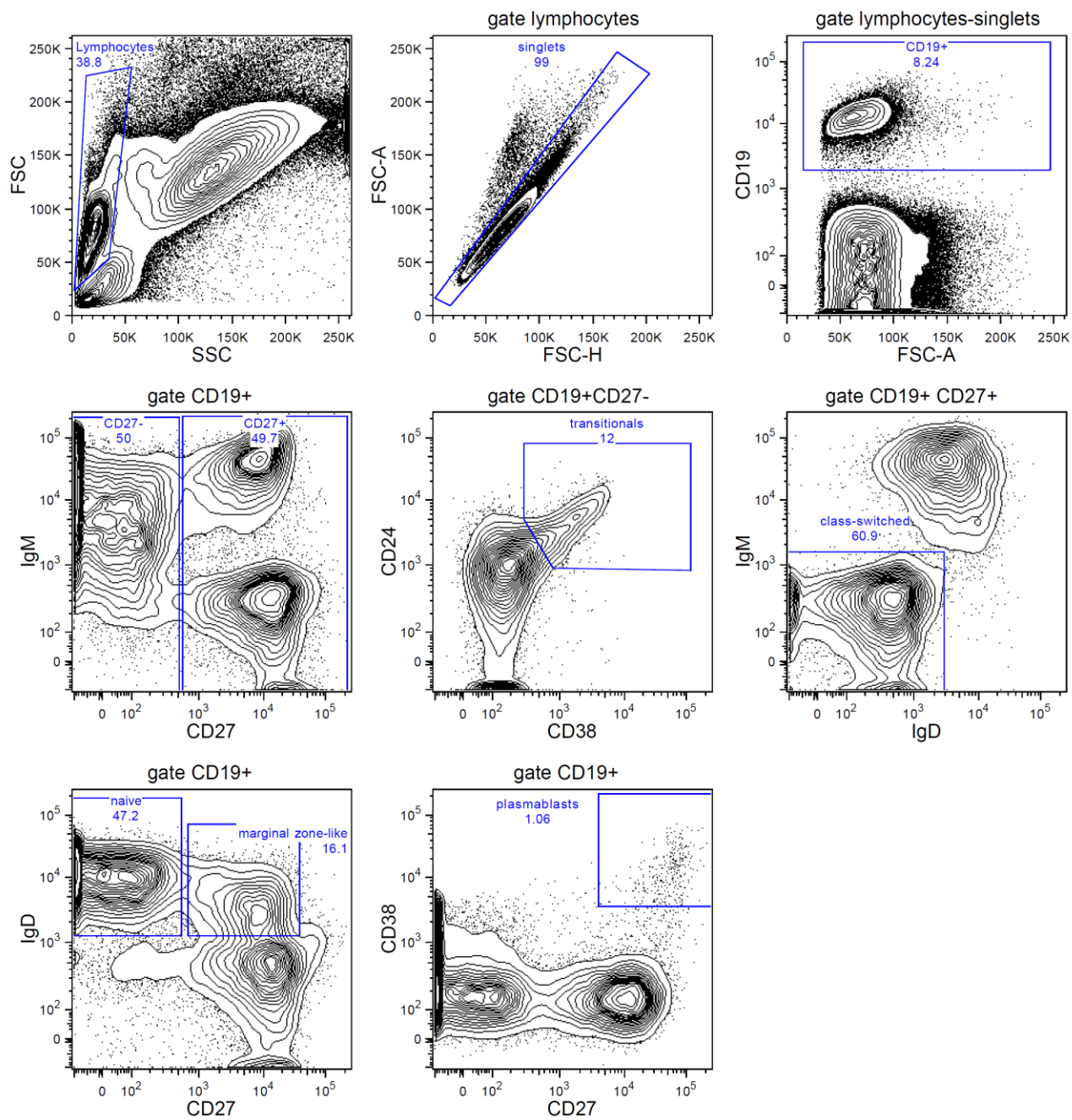


**Supplementary Figure 4.** Alteration of patient's mDC subpopulations. The patient's peripheral blood mononuclear cells (PBMC) showed, in two separated experiments, deficiency of both CD1c+ and CD141+ mDC subpopulations.

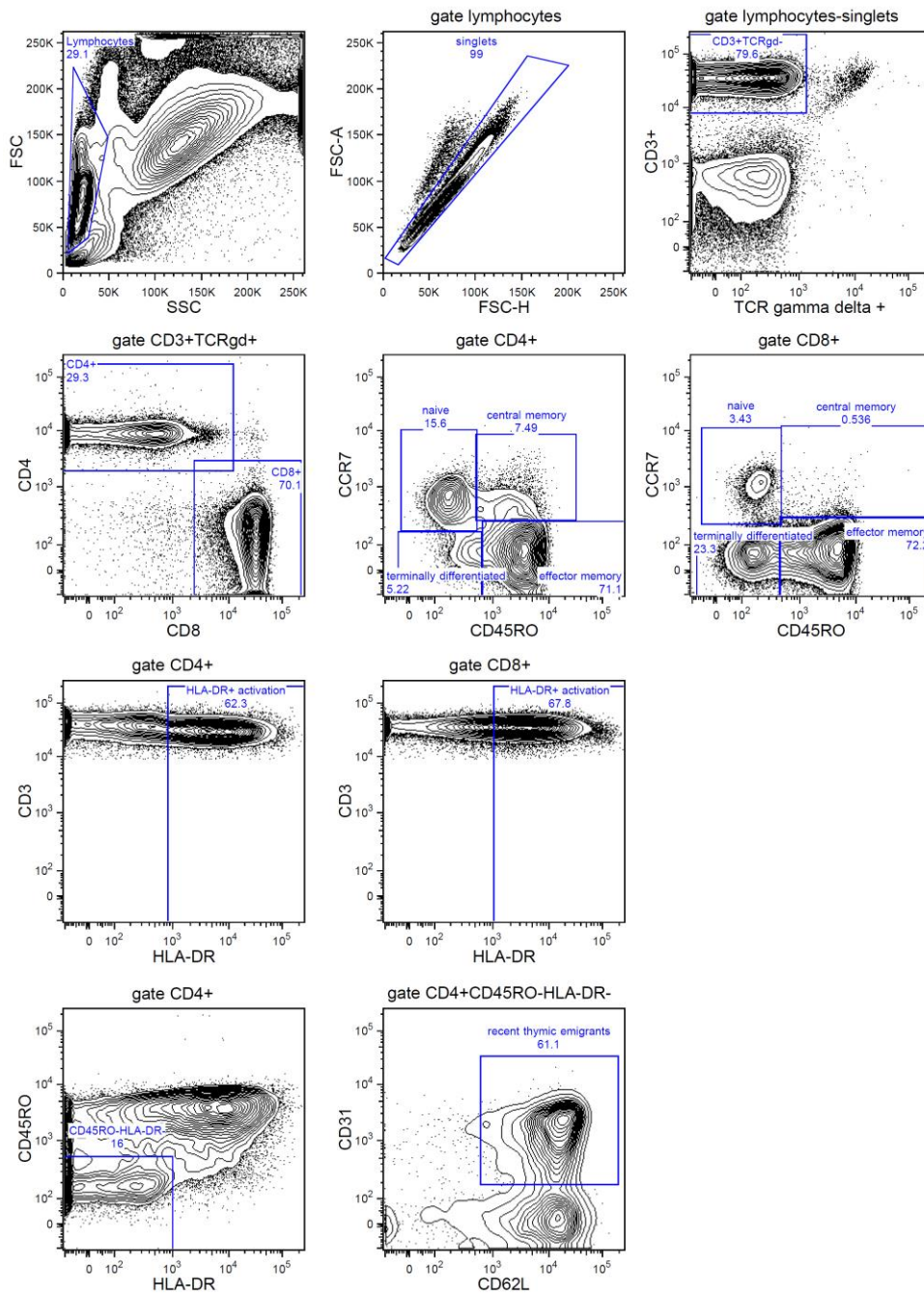




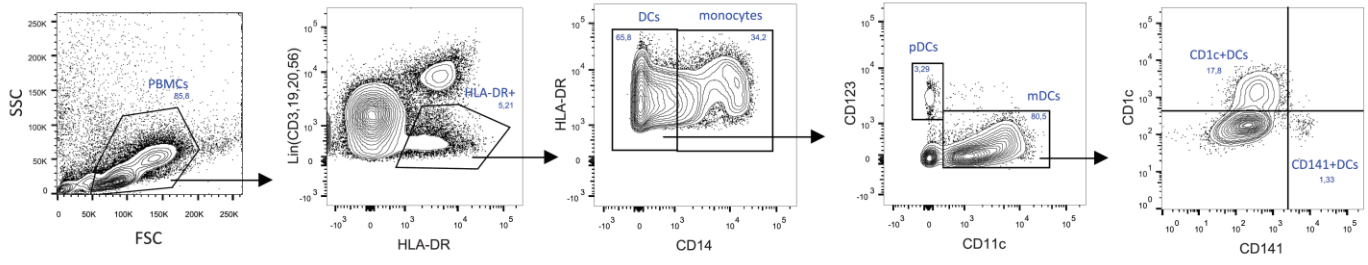
**Supplementary Figure 5. Minimal alteration of TLR4-induced cytokine production in the patient's cells. A.** The response of the patient's PBMC to TLR4 agonist lipopolysaccharide (LPS) did not differ from controls, as measured in the supernatants by Luminex. **B.** Flow cytometry revealed slightly reduced production of IL-6 in patient's monocytes upon LPS stimulation.



**Supplementary Figure 6. Gating strategy of B cells.** Independent healthy control is shown.



Supplementary Figure 7. Gating strategy of T cells. Patient's T cells are shown.



**Supplementary Figure 8. Gating strategy of DCs.** Independent healthy control is shown.

## Supplementary Methods

### Whole Exome Sequencing (WES)

The genomic DNA of the patient was analyzed on a NextSeq platform (Illumina, San Diego, CA) using the SureSelect Human Exon V6 kit (Agilent Technologies, Santa Clara, CA) and NextSeq 500/550 High Output v2 kit (Illumina) for sequencing. Library preparation and sequencing was performed according to the manufacturer's instructions.

### Variant calling and data analysis

Quality control of the raw data reads was performed using the FastQC program.<sup>1</sup> Alignment to the reference hg19 genome was carried out using BWA-MEM.<sup>2</sup> SAMtools was used to sort and index the alignments.<sup>3</sup> The Picard MarkDuplicates tool<sup>4</sup> was employed to mark and remove duplicates. The Vardict program<sup>5</sup> was used to determine genetic variants. The identified variants were annotated with Annovar tool.<sup>6</sup> Integrative Genomics Viewer (IGV)<sup>7</sup> was employed to visualize the read alignment and detected variants.

### DNA Sanger sequencing

Genomic DNA was used for PCR targeting of the *CASP8* area surrounding the p.P411L variant using the forward primer 5'-GCCCCATCTATGAGCTGAC-3' and the reverse primer 5'-CTCAGGCTCTGGCAAAGTGA-3'. The amplicons were sequenced using BigDye Terminator 3.1 Cycle Sequencing Kit (Thermo Fischer, Waltham, CA) on ABI Prism 3130 (Thermo Fischer) according to manufacturer's instructions.

### Immunophenotyping

Immunophenotyping of B-cell subpopulations was performed using antibody-fluorochrome conjugates CD27-Brilliant Violet (BV) 421, IgM-BV510, CD5-PE, IgD-PerCP-Cy5.5 (Biolegend, San Diego, CA, USA), CD19-PE-Cy7, CD24-APC-Alexa750 (Beckman Coulter (BC), Miami, FL), and CD38-FITC, CD21-APC (BD Biosciences (BD), San Jose, CA). The gating strategy of the B cells is shown in **Supplementary Figure 6**. Immunophenotyping of T-cell subpopulations was performed using CD27-BV421, CD4-BV510, HLA-DR-PerCP-Cy5.5, CD62L-BV421 (Biolegend), CD3-APC, TCRgd-PE-Cy7 (BD), CD8-APC-Alexa750 (BC), CD45RO-FITC, CD31-PE (Exbio, Vestec, Czech Republic), and CCR7-PE (Miltenyi Biotec, Bergisch Gladbach, Germany). The gating strategy of the T cells is shown in **Supplementary Figure 7**. Double-negative CD3+TCR $\alpha\beta$ +CD4-CD8- T cells were evaluated using CD45-PerCP, CD4-APC, CD8-Pacific Blue (Exbio), CD3-PE-Cy7, TCR $\alpha\beta$ -PE, and TCR $\gamma\delta$ -FITC (BC). For intracellular Ki-67 staining (Exbio), FACS Lyse and FACS Perm 2 buffers (BD) were used together with Ki-67-PE (Exbio) and custom made DuraClone tube (CD27-Pacific Blue, CD45RO-FITC, HLA-DR-PerC-Cy5.5, CCR7-PE-Cy7,

TCR $\alpha\beta$ -APC, CD8-APC-Alexa Fluor 750, and CD4-APC-Alexa Fluor 700, BC). Immunophenotyping of dendritic cells and monocytes was performed using Lin-FITC (CD3, CD19, CD20, CD56), CD16-Alexa Fluor 700, CD11c-APC, CD14-PE-DyLight594 (Exbio), HLA-DR-PerCP (BD), CD1c-BV510, CD141-BV421, and CD123-PE-Cy7 (Biolegend). The gating strategy of DCs is shown in **Supplementary Figure 8**.

### **Apoptosis**

FAS-induced T-cell apoptosis was examined as previously described by Lo et al.<sup>8</sup> PBMCs from the patient and controls were isolated using a Ficoll-Paque gradient (GE Healthcare, Uppsala, Sweden) and activated with phytohemagglutinin (PHA, 5  $\mu$ g/ml) and IL-2 (50 ng/ml) in complete medium (RPMI 1640 supplemented with 10% fetal bovine serum (FBS) and antibiotics) for 3 days. PHA and IL-2 were washed out, and the cells were cultured in complete medium with IL-2 (50 ng/ml) alone for 5 additional days. Apoptosis was induced with anti-FAS antibody (EOS9.1, Biolegend), and goat-anti-mouse antibody (BD) was used to crosslink the anti-FAS antibody. After 24 h, the cells were washed once in Annexin V Binding Buffer (Exbio), the cell pellet was supplemented with Annexin V-Dy647 (Exbio) and CD45-Pacific Orange (Exbio), CD27-BV421 (Biolegend), CD45RA-FITC, CD4-PerCP-Cy5.5, CD8-APC-H7 (BD), and CD3-ECD and CCR7-PE (Miltenyi), and incubated for 30 min on ice in the dark. The cell pellet was washed once in Annexin V Binding Buffer. The data were collected with an LSR II flow cytometer (BD) and analyzed with FlowJo software (BD). The cells were gated according to their forward scatter (FSC), side scatter (SSC), and CD45 positivity. The percentage of the apoptotic Annexin V-positive fraction was assessed for effector memory T cells (CD45<sup>+</sup>CD3<sup>+</sup>CD4<sup>+</sup>CD45RA<sup>-</sup>CCR7<sup>-</sup>CD27<sup>-</sup> cells). Fas-induced apoptosis = the ratio of apoptotic cells after 24 hours with and without anti-FAS stimulation. The Mann-Whitney U test was applied to assess the significance of the difference between the results of the patient and healthy control.

### **Lymphocyte activation and proliferation**

PBMCs from the patient and controls were isolated using a Ficoll-Paque gradient (GE Healthcare) and activated using anti-CD3/CD28 coated beads (Thermo Fisher) in complete medium with and without IL-2 (50 ng/ml). After 3 days, CD25 surface expression (BC) and Ki-67 intracellular expression (Exbio) were evaluated using an LSR II flow cytometer. For intracellular staining, FACS Lyse and FACS Perm 2 buffers (BD) were used. CellTrace Violet Cell Proliferation Kit (Thermo Fisher) was used according to manufacturer's instruction to detect proliferation of naïve (CD3<sup>+</sup>CD4<sup>+</sup> or CD8<sup>+</sup> CCR7<sup>+</sup>CD45RA<sup>+</sup>) and effector memory (CD3<sup>+</sup>CD4<sup>+</sup> or CD8<sup>+</sup> CCR7<sup>-</sup>CD45RA<sup>-</sup>) T cells 6 days upon anti-CD3/CD28 stimulation.

### **Intracellular signaling**

PBMCs obtained from the patient and healthy controls were stimulated using anti-CD3/CD28 coated beads (Thermo Fisher) or TNF $\alpha$  (Sigma Aldrich, St. Louis, MO) in complete medium at 37°C. Intracellular signaling was terminated using 4% formaldehyde at the indicated time points and the leukocytes were permeabilized using 0.1% Triton X-100. T-cell subpopulations were detected using CD45-Pacific Orange, CD8-Pacific Blue, CD45RA-FITC (Exbio), CD3-APC-Cy7 and CD4-PerCP-Cy5.5 (BD), and intracellular signaling was detected using anti-phospho-NF $\kappa$ B p65 (Ser536)-Alexa Fluor 647 (D3H1, Cell Signaling Technology, Danvers, MA).

### **Western Blotting**

PBMCs obtained from the patient and controls were lysed with lysis buffer containing 50 mM HEPES, 10 mM MgCl<sub>2</sub>, 140 mM NaCl, pH 8, supplemented with 0.1% Tween 20, 1% n-dodecyl beta-D-maltoside, 2 mM PMSF, proteinase inhibitors (no. P8340) and phosphatase inhibitors (no. P5736, Sigma Aldrich). The lysates were sonicated 4 times for 10 s, incubated for 60 min on ice and centrifuged at 21.255  $\times$  g for 10 min at 4°C. Supernatants were diluted 1:1 with Laemmli reducing sample buffer (Sigma Aldrich) and heated to 90°C for 5 min. Proteins were separated in SDS-PAGE gels and transferred onto nitrocellulose membranes (Bio-Rad, Hercules, CA). The membranes were blocked in 7.5% low-fat bovine milk in PBS with 0.05% Tween 20 at 8°C overnight. Anti-CASP8 (D35G2 and 1C12), cleaved CASP8 (Asp391), CASP3 (8G10), and cleaved CASP3 (Asp175) antibodies (Cell Signaling Technologies) were used together with peroxidase-conjugated secondary antibodies (Jackson Immunoresearch, West Grove, PA), and the SuperSignal West Pico and Femto Chemiluminescent Substrate (Thermo Fischer). Caspase cleavage was detected 4 h upon anti-FAS stimulation.

### **Cytokine production**

For intracellular cytokine detection, PBMCs were cultured in a 24-well microtiter plate at a concentration of 1 $\times$ 10<sup>6</sup>/well and stimulated using 50  $\mu$ g/ml poly(I:C) (Invivogen, San Diego, CA) and 1  $\mu$ g/ml LPS (Sigma Aldrich) for 7 h in the presence of 1  $\mu$ l/ml Brefeldin A (BD, added for 4 h). Cytokines were stained using IL-1 $\beta$ -PE (Thermo Fisher), IL-6-PE (Biolegend), and TNF $\alpha$ -PE (Exbio) and the data were collected using an Aria II flow cytometer (BD). The levels of IL-1 $\beta$ , IL-6, and TNF $\alpha$  in the supernatants were determined 24 h after the addition of TLR ligands using multiplex Luminex cytokine bead-based immunoassays (Millipore, Bedford, MA). Data were collected using the Luminex-100 system (Luminex, Austin, TX).

## TRECs

At the age of nine years the amount of T-cell receptor excision circles (TRECs) was determined by real-time PCR performed on 7500 Fast Real-Time PCR (Applied Biosystems) using TaqMan Fast Universal PCR MasterMix (2×) (Applied Biosystems) as described previously.<sup>9</sup>

## References to Supplementary Methods

1. Andrews S. FastQC: a quality control tool for high throughput sequence data. 2010. Available online at: <http://www.bioinformatics.babraham.ac.uk/projects/fastqc>.
2. Li H. Aligning sequence reads, clone sequences and assembly contigs with BWA-MEM. 2013. arXiv:1303.3997v1 [q-bio.GN].
3. Li H, Handsaker B, Wysoker A, et al. The Sequence Alignment/Map format and SAMtools. *Bioinformatics* 2009;25(16):2078-2079.
4. Available online at: <http://picard.sourceforge.net/>.
5. Lai Z, Markovets A, Ahdesmaki M, et al. VarDict: A novel and versatile variant caller for next-generation sequencing in cancer research. *Nucleic Acids Res* 2016;44(11):e108.
6. Wang K, Li M, Hakonarson H. ANNOVAR: Functional annotation of genetic variants from high-throughput sequencing data. *Nucleic Acids Res* 2010;38(16):e164.
7. Robinson JT, Thorvaldsdóttir H, Winckler W, et al. Integrative genomics viewer. *Nat Biotechnol* 2011;29(1):24–26.
8. Lo B, Ramaswamy M, Davis J, et al. A rapid ex vivo clinical diagnostic assay for Fas receptor-induced T lymphocyte apoptosis. *J Clin Immunol* 2013;33(2):478–488.
9. Sottini A, Ghidini C, Zanotti C, et al. Simultaneous quantification of recent thymic T-cell and bone marrow B-cell emigrants in patients with primary immunodeficiency undergone to stem cell transplantation. *Clin Immunol* 2010;136(2):217-227.